This article has been accepted for publication in a future issue of this journal, but has not been fully edited. Content may change prior to final publication. Citation information: DOI 10.1109/JLT.2018.2851918, Journal of Lightwave Technology

Gain Switching of Monolithic 1.3 μm InAs/GaAs Quantum Dot Lasers on Silicon

Constanze Hantschmann, Peter P. Vasil'ev, Siming Chen, *Member, IEEE,* Mengya Liao, *Student Member, IEEE,* Alwyn J. Seeds, *Fellow, IEEE,* Huiyun Liu, *Senior Member, IEEE,* Richard V. Penty, *Senior Member, IEEE,* and Ian H. White, *Fellow, IEEE*

***Abstract*— We report the first demonstration of gain-switched optical pulses generated by continuous-wave 1.3 µm InAs/GaAs quantum dot (QD) broad-area lasers directly grown on silicon (Si). The shortest observed pulses have typical durations between 175 ps and 200 ps with peak output powers of up to 66 mW. By varying the drive current pulse width and amplitude systematically, we find that the peak optical power is maximized through sufficiently long high-amplitude drive pulses, whereas shorter drive pulses with high amplitudes yield the narrowest achievable pulses. A three-level rate equation travelling wave model is used for the simulation of our results in order to gain a first insight into the underlying physics and the laser parameters responsible for the observed behavior. The simulations indicate that limited gain from the InAs quantum dots and a very high gain compression factor are the main factors contributing to the increased pulse width. As the optical spectra of the tested broad-area QD laser give clear evidence of multi-transverse mode operation, the laser's dynamic response could be additionally limited due to transversal variations of the gain, carrier density, and photon density over the 50 µm wide laser waveguide.**

***Index Terms*— Optical pulses, photonic integrated circuits, quantum dot lasers, semiconductor device modeling, silicon photonics**

I. Introduction

THE continuing demand for increased bandwidth in high-performance computing data centers poses a challenge for research and industry. While the demand has driven the development of faster components throughout the whole communication link, it has also led to studies on higher levels of system integration with greater capacity and reduced component cost [1], [2]. Merging optical and electrical components on an integrated optoelectronic circuit on a silicon-based platform or realizing a silicon (Si) photonics chip for optical on-chip communications are, therefore, highly attractive longer-term solutions [3]-[7].

Monolithic on-chip light sources represent essential components for this undertaking, but due to Si's indirect energy band structure, high-gain III/V semiconductor lasers, such as those using the GaAs system, have to be used [8], [9]. Regrettably, the direct growth of GaAs-based lasers on Si substrates is hampered by the lattice mismatch of GaAs and Si [10]-[12] and thermal expansion coefficients [11]-[13]. In recent years, however, substantial advances have been achieved in the monolithic integration of III/V devices on Si and recent research has produced impressive results for monolithic 1.3 µm InAs/GaAs quantum dot (QD) lasers on miscut Si without intermediate Ge or GaP buffers [14]-[15] as well as on on-axis (001) Si [16]-[22]. Active material systems using InAs QDs have turned out to have an enhanced tolerance to lattice defects arising from the strained GaAs-Si interface [14]-[17], and, consequently, can yield good device performance with the use of carefully tailored growth conditions and dislocation filters [13], [23]. This has resulted in successful continuous-wave (cw) operation at temperatures over 100 °C [15], low threshold current densities of 62.5 A/cm^2 [14] and an absolute value as small as 6.2 mA, cw optical output power of 185 mW, and extrapolated lifetimes of longer than one million hours [20]. Recent publications report even the first direct modulation and mode-locking of cw 1.3 µm QD lasers on GaP/(001) Si, demonstrating a small-signal modulation bandwidth of 6.5 GHz and large-signal modulation at 12.5 Gb/s [21], and 490 fs pulse generation at a repetition rate of 31 GHz [22]. Monolithic 1.3 µm QD lasers on Si substrates are thus one of the best candidates for applications such as in integrated optoelectronic or silicon photonic circuits. They are also attractive as Si-based CMOS growth and fabrication processes have the highest level of maturity of all semiconductor materials, enabling low-cost and large-area fabrication for high-volume applications [5], [7], [24]. Since future communication systems have to be scalable as well as cost-competitive [25], and laser growth on III/V substrates is relatively expensive, cost is another key potential advantage for Si-based lasers in optical communication applications. However, much remains to be learnt about the physical properties of monolithic 1.3 µm QD lasers on Si

Manuscript received March 24 2018. This work is supported by UK EPSRC at the University of Cambridge and at University College London (UCL Grant No. EP/J012904/1 and EP/J012815/1). C. Hantschmann's Ph.D. studies are funded by Qualcomm Inc.. S.-M. Chen's Research Fellowship is funded by the Royal Academy of Engineering under Reference No. RF201617/16/28.

C. Hantschmann, P. P. Vasil'ev, R. V. Penty, and I. H. White are with the Centre for Photonic Systems, Department of Engineering, University of Cambridge, Cambridge CB3 0FA, UK. (e-mail: cb893@cam.ac.uk; pv261@cam.ac.uk, rvp11@cam.ac.uk, ihw3@cam.ac.uk).

S.-M. Chen, M. Liao, A. J. Seeds, and H. Liu are with the Department of Electronic and Electrical Engineering, University College London, London WC1E 7JE, UK. (e-mail: siming.chen@ucl.ac.uk, mengya.liao@ucl.ac.uk, a.seeds@ucl.ac.uk, huiyun.liu@ucl.ac.uk).

P. P. Vasil'ev is also associated with the PN Lebedev Physical Institute, Moscow 119991, Russia.

0733-8724 (c) 2018 IEEE. Personal use is permitted, but republication/redistribution requires IEEE permission. See http://www.ieee.org/publications_standards/publications/rights/index.html for more information.

This article has been accepted for publication in a future issue of this journal, but has not been fully edited. Content may change prior to final publication. Citation information: DOI 10.1109/JLT.2018.2851918, Journal of Lightwave Technology

substrates, and in particular the dynamic properties of this novel type of semiconductor laser. Whereas few experimental results start to become available [21], [22], no comprehensive theoretical study investigating the dynamics of Si-based QD lasers has been published yet. This paper is, therefore, a first step towards a rigorous analysis of the high-speed characteristics of monolithic QD lasers on Si substrates to investigate existing performance limitations, and to seek pathways of overcoming them.

Gain-switching is a simple means of gaining insight into the basic dynamics of a semiconductor laser. A very short optical pulse is generated by driving the laser with a short, high-amplitude electrical pulse, so that the stimulated emission is stopped after the first relaxation oscillation peak [26]. In this paper, we report, to the best of our knowledge, the first demonstration of gain-switched optical pulses generated by monolithic 1.3 µm InAs/GaAs QD lasers on Si substrates. The shortest observed pulses have typical widths between 175 ps and 200 ps with peak powers of up to 66 mW. These are presented together with a study of the dependence of the peak optical power and optical pulse duration on the electrical drive conditions. A spatiotemporal travelling wave model based on three-level rate equations and coupled wave equations is used to simulate the optical pulses, allowing an insight into the underpinning laser parameters.

II. Device Structure

The QD laser used for our measurements is based on the device structure presented in [14]. The laser structure is grown on a (001) Si substrate offcut towards the [011] plane to avoid the formation of antiphase boundaries resulting from the growth of polar GaAs on the non-polar Si substrate [27]. Initially, a thin AlAs nucleation layer is grown that prevents the start of a three-dimensional growth mode. The subsequent 1 µm thick GaAs layer inhibits some of the dislocations emerging at the GaAs-Si interface. The remaining defects are further reduced in the following dislocation filter, which consists of four periods of InGaAs/GaAs strained-layer superlattices each with 300 nm GaAs spacer layers. The resulting GaAs pseudo-substrate has a dislocation density of only ~10^5 cm^{-2}. The GaAs-based active region is grown sandwiched between the 1.4 µm *n*- and *p*-doped cladding layers as shown schematically in Fig. 1.

The active layers are embedded into a 140 nm undoped GaAs layer and consist of 5 In(Ga)As dots-in-a-well (DWELL) periods. The DWELL layers have a QD density of approximately 3×10^{10} cm^{-2} and are separated by 50 nm thick GaAs spacer layers. The top electrical Ti/Pt/Au contact is made on a 300 nm *p*-doped GaAs layer grown on top of the *p*-cladding, while the Ni/GeAu/Ni/Au *n*-contact is made in the lower *n*-doped layer. The epitaxial material is then fabricated into broad-area lasers with as-cleaved facets. For good thermal dissipation, the laser bar is mounted on a copper heatsink and then contacted using wire bonds.

III. Methods and Experimental Results

The device under test is a 3.1 mm-long broad-area laser with a 50 µm-wide waveguide. For the static characterization, the laser is operated under cw current injection at room temperature

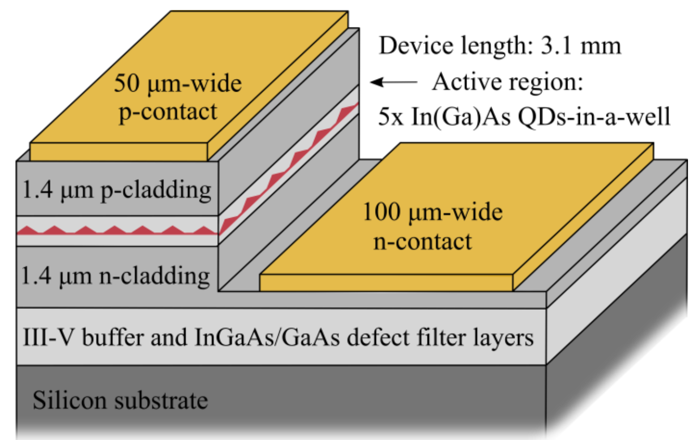

Fig. 1. Device structure of the monolithic InAs/GaAs QD laser on a Si substrate used for the gain-switching experiments.

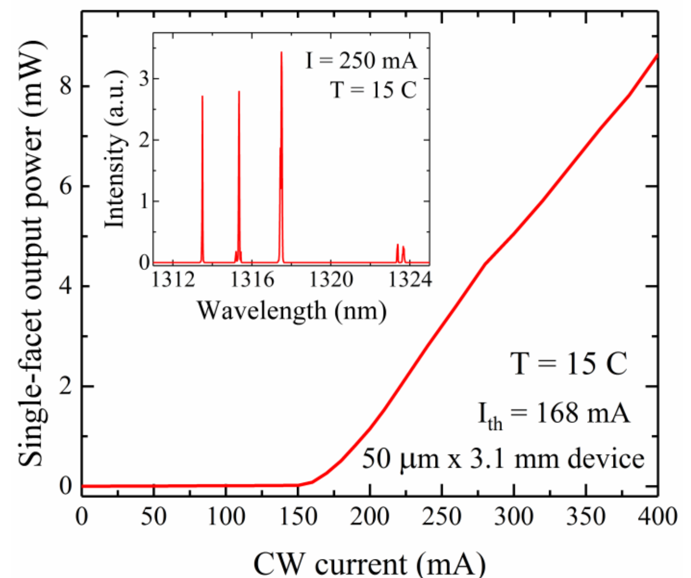

Fig. 2. *LI* characteristic of the 50 µm × 3.1 mm QD laser recorded under cw conditions at 15 °C. The inset shows the multimode laser spectrum at 250 mA.

with the heatsink temperature set to 15 °C. Under these conditions, the laser's light-current (*LI*) characteristic shows a threshold current of 168 mA, as depicted in Fig. 2. The forward resistance obtained from the voltage-current curve is 2.5 Ω.

The gain-switching experiments are performed using a circuit producing a nanosecond long electrical pulse of variable amplitude and duration without prebias to drive the QD laser at a frequency of 100 kHz. The exact amplitude and pulse duration can be adjusted to generate the shortest possible optical pulse, which is then observed on an oscilloscope. It is observed that the peak optical power increases as the drive amplitude increases, while increasing the current pulse width is a means of maximizing the peak optical power for a given current, as shown in Fig. 3(a) and (b). Conversely, the narrowest achievable optical pulse duration decreases with rising current amplitude. The dependence of the optical pulse width on the electrical pulse width depends on the exact operation point of the laser. As illustrated in Fig. 3(c), a too narrow drive pulse does not contain sufficient carriers to switch on the laser

0733-8724 (c) 2018 IEEE. Personal use is permitted, but republication/redistribution requires IEEE permission. See http://www.ieee.org/publications_standards/publications/rights/index.html for more information.

This article has been accepted for publication in a future issue of this journal, but has not been fully edited. Content may change prior to final publication. Citation information: DOI 10.1109/JLT.2018.2851918, Journal of Lightwave Technology

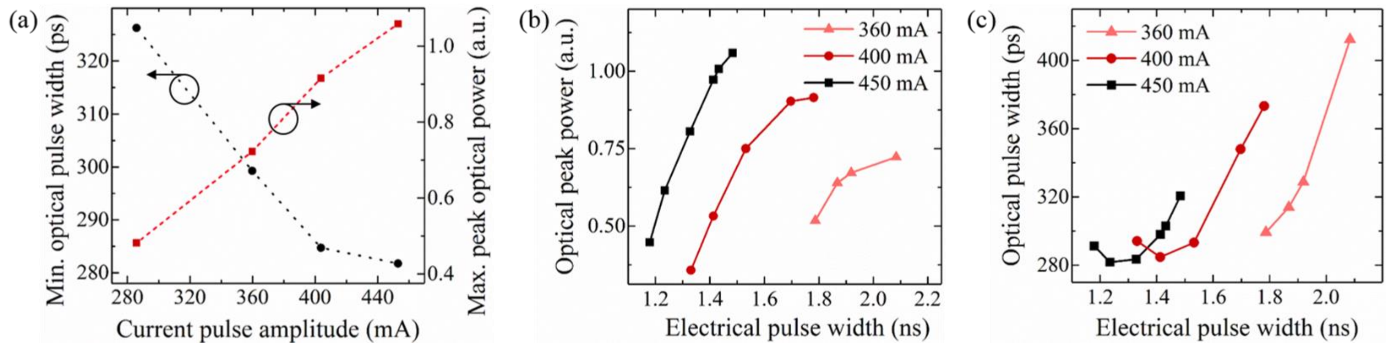

Fig. 3. Systematic study of the characteristics of gain-switched pulses from the 50 μm × 3.1 mm QD laser driven at 100 kHz without prebias. (a) Minimum optical pulse width and maximum peak optical amplitude plotted versus the drive pulse amplitude. (b) Peak optical power against the current pulse width for three different current amplitudes. (c) Optical pulse width against the current pulse width for the same three current amplitudes.

powerfully enough to obtain a sharp gain-switched pulse, whereas an excessively long drive pulse results in a broadening of the gain-switched pulse due to surplus carrier injection.

The shortest optical pulse widths of 200 ps to 175 ps are obtained using high current amplitudes of 500 to 750 mA. Two examples of pulses measured at these currents are shown in Fig. 4. From the measurement of the average optical power of the signal using a large-area detector, a peak optical power of about 66 mW is estimated. While the pulse rise times of the shortest obtained pulses are about 95 ps to 140 ps, their longer fall times of typically 300 ps to 340 ps limit the pulse width. For the 3.1 mm laser length and a resulting roundtrip time of approximately 74 ps, the measured pulse widths correspond to a few laser roundtrip times, which is typical of gain switching [28]. Compared with pulse widths achieved with shorter high-gain quantum well or bulk lasers of the order of 10 ps to 15 ps [29]-[34], the pulses produced by the monolithic QD lasers on Si substrates are one order of magnitude longer, which is mainly a result of the lower gain and the long cavity length necessary to compensate for that. No laser design optimization has been performed as yet, so we expect to measure shorter pulses by increasing the number of active layers and optimizing the photon lifetime combined with a narrow ridge-waveguide laser design [35].

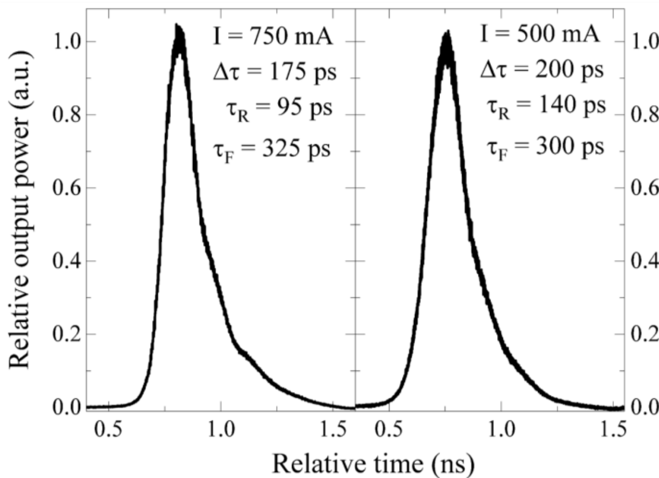

Fig. 4. Two normalized gain-switched pulses from the QD lasers with a current amplitude of 750 mA (left) and 500 mA (right). Δτ, τ_r, and τ_F denote the optical pulse width at half height and the pulse rise and fall time, respectively. The electrical pulse duration, rise time, and fall time are about 0.85 ns, 0.45 ns, and 0.5 ns for I = 750 mA, and 1.1 ns, 0.6 ns, and 0.95 ns for I = 500 mA.

IV. Theoretical Model and Simulations

In order to gain insight into the underlying physics of the dynamic properties of monolithic QD lasers on Si substrates, a three-level rate equation travelling wave model is used to simulate our experiments [36], [37]. Longitudinal spatial effects are specifically included by discretizing the laser into 5 μm long sections for which the gain, the carrier densities, and the forward and reverse travelling fields are calculated at each time step ($\Delta t = 60$ fs). Since the model provides one-dimensional spatial resolution only, transverse mode effects are not considered in the simulations. The carrier densities $N_{WL}(z,t)$, $N_{ES}(z,t)$, and $N_{GS}(z,t)$ in the wetting layer (WL), QD excited state (ES) and ground state (GS) respectively are computed based on a set of coupled differential equations describing current injection into the WL volume V_{WL}, the carrier capture and intradot relaxation into the QD GS volume V_D, thermal escape, carrier losses, and lasing from the GS [37]. An explanation of the symbols used and their values can be found in Table 1.

$$\frac{\partial N_{WL}}{\partial t} = \frac{\eta I}{eV_{WL}} + \frac{V_D}{V_{WL}}\frac{N_{ES}}{\tau_{esc}^{ES}} - \frac{N_{WL}(1-f_{ES})}{\tau_c} - \frac{N_{WL}}{\tau^{WL}} \quad (1)$$

$$\frac{\partial N_{ES}}{\partial t} = \frac{V_{WL}}{V_D}\frac{N_{WL}(1-f_{ES})}{\tau_c} + \frac{N_{GS}(1-f_{ES})}{\tau_{esc}^{GS}} - \frac{N_{ES}}{\tau_{esc}^{ES}} - \frac{N_{ES}(1-f_{GS}^{e})}{\tau_0} - \frac{N_{ES}}{\tau^{ES}} \quad (2)$$

$$\frac{\partial N_{GS}}{\partial t} = \frac{N_{ES}(1-f_{GS}^{e})}{\tau_0} - \frac{N_{GS}(1-f_{ES})}{\tau_{esc}^{GS}} - v_{gr} g S - \frac{N_{GS}}{\tau^{GS}} \quad (3)$$

The electron dynamics are agreed to be the limiting factor for the carrier dynamics, as the hole dynamics are fast due to their narrow energy spacing and their higher effective mass [38], [39]. For this reason, the hole dynamics are not taken into account separately in this model. In addition, only one ES and one GS are considered. Pauli blocking and the 4-fold and 2-fold ES and GS energy degeneracy are included using the ES and GS occupation probabilities $f_{ES} = \frac{N_{ES}V_{Dot}}{4}$ and $f_{GS}^{e} = \frac{N_{GS}V_{Dot}}{2}$, which are calculated using the volume V_{Dot} of an individual QD [40]. The QD gain is parametrized via the maximum material gain g_{mat}^{max}, the electron and hole GS occupation probabilities $f_{GS}^{e,h}$, and the phenomenological gain compression factor ε.

0733-8724 (c) 2018 IEEE. Personal use is permitted, but republication/redistribution requires IEEE permission. See http://www.ieee.org/publications_standards/publications/rights/index.html for more information.

This article has been accepted for publication in a future issue of this journal, but has not been fully edited. Content may change prior to final publication. Citation information: DOI 10.1109/JLT.2018.2851918, Journal of Lightwave Technology

$$g(N_{GS}, S) = \frac{g_{mat}^{max}\left(f_{GS}^{e}+f_{GS}^{h}-1\right)}{1+\varepsilon S} \quad (4)$$

The material gain and the modal gain are linked via the confinement factor Γ according to $g_{mod} = \Gamma g_{mat}^{max}$, which has to be considered in (5) and (6) [37], [41]. The forward and reverse propagating electric fields F and R are then calculated using a pair of field equations including gain g, loss α_i, phase detuning δ, and spontaneous noise $i_{spf,r}$.

$$\left(\frac{1}{v_{gr}}\frac{\partial}{\partial t}+\frac{\partial}{\partial z}\right)F(z,t) = (\Gamma g-\alpha_i-i\delta)F(z,t)+i_{spf}(z,t) \quad (5)$$

$$\left(\frac{1}{v_{gr}}\frac{\partial}{\partial t}-\frac{\partial}{\partial z}\right)R(z,t) = (\Gamma g-\alpha_i-i\delta)R(z,t)+i_{spr}(z,t) \quad (6)$$

Based on this, the photon density is calculated by

$$S(z,t) = |F(z,t)|^2+|R(z,t)|^2, \quad (7)$$

which is why g and α_i have to be scaled with a factor ½ in the numerical implementation of the field equations. The photon density is then coupled back into the carrier rate equations. The shape of the QD gain spectrum is modelled by applying a digital Lorentzian filter with the spectral response

$$H(f) = \frac{g\cdot\cos(\pi f\Delta t)}{\cos(\pi f\Delta t)+iK\sin(\pi f\Delta t)} \quad (8)$$

to (5) and (6). The material gain bandwidth $\Delta\lambda$ around the center wavelength λ_0 is introduced by the filter parameter

$$K = \frac{\lambda_0^2}{\pi c\Delta t\cdot\Delta\lambda}, \quad (9)$$

where c is the speed of light [42].

Fig. 5 shows the simulations of gain-switched pulses at current pulse amplitudes of 500 mA and 750 mA in comparison to the experimentally obtained pulses. A super-Gaussian current pulse with an exponentially decaying trailing edge is used to represent a realistic input source. At both current settings, the modelled pulses reproduce the dynamics of their experimental counterparts well. The respective simulation parameters in Table 1 are chosen based on common values for InAs/GaAs QD lasers found in the literature and then adjusted to reproduce our experimental data. The fact that hardly any of these parameters have been investigated for Si-based QD lasers highlights the importance of performing detailed measurements supported by numerical modelling for the parameter extraction. In seeking to fit the theory to experimental measurement, two key parameters have been found to be particularly important. Specifically, a lower gain and a very high gain compression factor are the parameters that principally contribute to a slower pulse rise time and a longer pulse duration. These also limit the high-speed performance of QD lasers in general. In particular, the high gain compression factor of 9×10^{-16} cm^3, which is more than one order of magnitude higher than typical QW gain compression factors [43], causes a broadening of the pulse and a slowly decaying trailing edge. This reflects gain saturation and carrier transport effects as well as contributions from multi-transverse and multi-longitudinal mode operation [41], [43]-[44] and is expected to limit the small-signal and large-signal modulation response. For the simulation of the laser's LI curve under cw injection, a low modal gain of about 14 cm^{-1}, which is comparable with the threshold gain of 13.8 cm^{-1} reported in [20], yields a good match with the experimental result. However, a higher value is required when modelling the laser performance at pulsed operation. To simulate the measured gain-switched pulses, a modal gain on the order of 20 cm^{-1} is, therefore, needed to reproduce the experimental pulse rise times. Yet after all it is important to bear in mind that the transverse variations occurring over the width of the 50 µm waveguides in the local gain, the carrier density, and the photon density, allow for substantial variations in the observed device performance, and thus in the associated simulation parameters [45], [46]. It is, therefore, expected that greater confidence about laser parameters likely to be obtained in Si-based 1.3 µm QD lasers can be achieved through further experiments with narrow ridge-waveguide lasers.

V. Discussion

While some laser parameters are very difficult to influence, for instance the intrinsic gain compression factor or the QD density of the large InAs dots required for emission at 1.3 µm [47], others are more readily tailored through changes in the laser design or the growth technique. The simulation results show that a first practical means of shortening the pulse duration is using a higher number of QD layers for a direct increase of the modal gain. A recent demonstration of conventional InAs QD high-speed lasers on GaAs, for instance,

TABLE I
Simulation Parameters used for Fig. 5

Laser length $L = 3.1$ mm	Facet reflectivity $R_l = R_l = 0.33$
Waveguide width $W = 50$ µm	Group velocity $v_{gr} = 8.4\times10^7$ m/s
Gain bandwidth $\Delta\lambda = 15$ nm	QD density $\rho = 2.5\times10^{10}$ cm^{-2}
Number of QD layers = 5	WL lifetime $\tau^{WL} = 0.5$ ns
GS escape time $\tau_{esc}^{GS} = 18$ ps	ES, GS lifetime $\tau^{ES,GS} = 0.8$ ns
ES escape time $\tau_{esc}^{ES} = 44$ ps	Intradot relaxation time $\tau_0 = 500$ fs
Carrier capture time $\tau_c = 1$ ps	Confinement factor $\Gamma = 5\times10^{-4}$
Injection efficiency $\eta = 0.25$	Elementary charge $e = 1.6\times10^{-19}$ C
Gain compression factor $\varepsilon = 9\times10^{-16}$ cm^3	GS hole occupation probability $f_{GS}^{h} = 0.5$
Modal gain $g_{mod} = 20.5$ cm^{-1}	Spontaneous emission coupling factor
Optical loss $\alpha_i = 3$ cm^{-1}	$\beta = 10^{-4}$

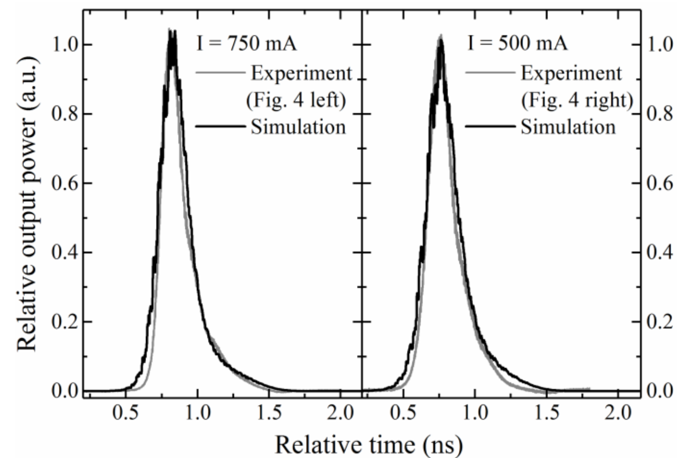

Fig. 5. Modelled gain-switched pulses (black) using the parameters shown in Table 1 in comparison to the experimental pulses (grey) displayed in Fig. 4. To allow better comparison, all pulses are normalized. Super-Gaussian current pulses with amplitudes of 750 mA (left) and 500 mA (right) and an exponentially decaying trailing edge are used to account for the imperfections of a realistic input source.

0733-8724 (c) 2018 IEEE. Personal use is permitted, but republication/redistribution requires IEEE permission. See http://www.ieee.org/publications_standards/publications/rights/index.html for more information.

This article has been accepted for publication in a future issue of this journal, but has not been fully edited. Content may change prior to final publication. Citation information: DOI 10.1109/JLT.2018.2851918, Journal of Lightwave Technology

incorporates 10 QD layers in the active region [48]. For such a ten-layer QD active region, the simulation predicts a shortening of the gain-switched pulse down to about 130 ps if the available gain increases by 50 %, and pulse durations between 90 and 110 ps if the modal gain is doubled.

Whereas for the case of as-cleaved facets the long cavity is crucial to maintain laser operation, higher gain would also offer more flexibility for an adjusted photon lifetime

$$\tau_{ph} = \frac{1}{v_{gr}(\alpha_i+\alpha_m)} . \quad (10)$$

Similar to the modulation bandwidth measured in small-signal modulation experiments, gain-switched pulses can be sped up by reducing the photon lifetime. Since the mirror loss α_m is directly related to the laser length and the facet reflectivities through

$$\alpha_m = \frac{1}{L}\ln\left(\frac{1}{\sqrt{R_1 R_2}}\right) , \quad (11)$$

the use of shorter cavities in combination with low facet reflectivities would allow shorter pulses to be generated [28], [49].

A different approach is the utilization of a high-reflection coating at the rear facet, so that the cavity length can be reduced. Although this does not necessarily reduce the photon lifetime, the cavity length reduction is accompanied by an increase of the laser efficiency, which could result in shorter pulses as well [49]. The fabrication of narrow ridge-waveguide lasers rather than broad-area devices would be another simple step resulting in a number of effects beneficial for the device performance, such as lower threshold currents which are accompanied by reduced heating effects and consequently reduced carrier losses, a higher current injection efficiency, and more homogeneous pumping of the QDs associated with a more homogeneous optical distribution.

Although epitaxial improvements tend to be more challenging, the pulse width could also be reduced by a number of other methods such as further reducing the optical losses, by optimizing the QD growth so that a higher uniformity and narrower gain bandwidth is achieved, by *p*-doping the active region to enhance the carrier transport and to increase the GS hole occupation probability and thus the gain [50], or by optimizing the carrier transport into the active region by narrower spacer layers [48]. The high gain compression factor used in the simulations suggests that especially improving the carrier transport in the thick QD active region could be a key factor in developing Si-based QD lasers suitable for optical communications. Based on these future developments, we expect, therefore, to observe an improved dynamic performance with the next generation of QD lasers on Si.

VI. Conclusion

In conclusion, we have presented an experimental and theoretical study of gain-switched optical pulses generated by monolithic 1.3 µm InAs/GaAs QD broad-area lasers. The shortest obtained pulses have typical durations between 175 ps and 200 ps and a maximum peak power of up to 66 mW. Systematic measurements show that optical pulses with higher power and shorter durations are achieved by increasing the drive pulse amplitudes, whereas there is a trade-off between maximizing the optical power and minimizing the respective pulse width for the electrical pulse width. A rate equation based travelling wave model has been used to simulate the shortest experimental pulses in order to obtain a set of laser parameters that is able to model the behavior of these lasers. In general, a good agreement between experiment and theory is found. The results show that, despite the great advances in the performance of Si-based QD lasers over the last years, significant improvements can be made in order to optimize their dynamic properties for optical communication applications. While the dynamic performance of GaAs-based InAs QD lasers is inherently limited by strong gain compression, monolithic InAs QD lasers on Si in particular suffer additionally from the defects introduced by the GaAs-Si interface. The primary concern should, therefore, be providing higher gain and reducing the large gain compression factor, which is most likely achievable by more active layers and *p*-doping the active region. In combination with some laser geometry modifications, this will bring monolithic growth of 1.3 µm QD lasers on Si substrates a major step closer towards applications in integrated optoelectronic or Si photonic circuits.

References

[1] M. Dagenais, R. F. Leheny, and J. Crow, “Preface,” in *Integrated Optoelectronics,* 1st ed., San Diego, CA, USA: Academic Press, 2013, pp. xiii–xv.

[2] O. Wada, “Optoelectronic Integration - Overview,” in *Optoelectronic Integration: Physics, Technology and Applications,* Norwell, MA, USA: Kluwer Academic Publishers, 1994, pp. 1–16.

[3] M. Liao, S.-M. Chen, S. Huo, S. Chen, J. Wu, M. Tang *et al.,* “Monolithically integrated electrically pumped continuous-wave III-V quantum dot light sources on silicon,” *IEEE J. Sel. Top. Quantum Electron.*, vol. 23, no. 6, pp. 1–10, Nov-Dec. 2017.

[4] M. Liao, S.-M. Chen, M. Tang, J. Wu, W. Li, K. Kennedy *et al.,* “Integrating III-V quantum dot lasers on silicon substrates for silicon photonics,” in *Proc. of SPIE Vol. 10108,* San Francisco, CA, USA, 2017, pp.10108A-1–101081A-8.

[5] A. Y. Liu, S. Srinivasan, J. Norman, A. C. Gossard, and J. E. Bowers, “Quantum dot lasers for silicon photonics,” *Photon. Res.*, vol. 3, no. 5, pp. B1–B9, Oct. 2015.

[6] R. Soref, “The past, present, and future of silicon photonics,” *IEEE J. Sel. Top. Quantum Electron.*, vol. 12, no. 6, pp. 1678–1687, Nov-Dec. 2006.

[7] A. Lee, Q. Jiang, M. Tang, A. J. Seeds, and H. Liu, “Continuous-wave InAs/GaAs quantum-dot laser diodes monolithically grown on si substrate with low threshold current densities,” *Opt. Express*, vol. 20, no. 20, pp. 22181–22187, Sep. 2012.

[8] A. D. Lee, Q. Jiang, M. Tang, Y. Zhang, A. J. Seeds, and H. Liu, “InAs/GaAs quantum-dot lasers monolithically grown on Si, Ge, and Ge-on-Si substrates,” *IEEE J. Sel. Top. Quantum Electron.*, vol. 19, no. 4, pp. 1901107–1901107, July-Aug. 2013.

[9] D. Liang, and J. E. Bowers, “Recent progress in lasers on silicon,” *Nat. Photonics*, vol. 4, pp. 511–517, Aug. 2010.

[10] C.-H. Choi, R. Ai, and S. A. Barnett, “Suppression of three-dimensional island nucleation during GaAs growth on Si (100),” *Phys. Rev. Lett.*, vol. 67, no. 20, pp. 2826–2829, Nov. 1991.

[11] K. K. Linder, J. Phillips, O. Oasaimeh, X. F. Liu, S. Krishna, P. Bhattacharya *et al.,* “Self-organized $In_{0.4}Ga_{0.6}As$ quantum-dot lasers grown on Si substrates,” *Appl. Phys. Lett.*, vol. 74, no. 10, pp. 1355–1357, Mar. 1999.

[12] Z. Mi, J. Yang, P. Bhattacharya, and D. L. Huffaker, “Self-organised quantum dots as dislocation filters: the case of GaAs-based lasers on silicon,” *Electron. Lett.*, vol. 42, no. 2, pp. 121–123, Jan. 2006.

[13] M. Tang, S. Chen, J. Wu, Q. Jiang, K. Kennedy, P. Jurczak *et al.,* “Optimizations of defect filter layers for 1.3-µm InAs/GaAs quantum-dot lasers monolithically grown on Si substrates,” *IEEE J. Sel. Top. Quantum Electron.,* vol. 22, no. 6, pp. 50–56, Nov-Dec. 2016.

0733-8724 (c) 2018 IEEE. Personal use is permitted, but republication/redistribution requires IEEE permission. See http://www.ieee.org/publications_standards/publications/rights/index.html for more information.

This article has been accepted for publication in a future issue of this journal, but has not been fully edited. Content may change prior to final publication. Citation information: DOI 10.1109/JLT.2018.2851918, Journal of Lightwave Technology

[14] S. Chen, M. Liao, M. Tang, J. Wu, M. Martin, T. Baron *et al.,* "Electrically pumped continuous-wave III–V quantum dot lasers on silicon," *Nat. Photonics*, vol. 10, pp. 307–311, Mar. 2016.

[15] A. Y. Liu, C. Zhang, J. Norman, A. Snyder, D. Lubyshev, J. M. Fastenau *et al.,* "High performance continuous wave 1.3 µm quantum dot lasers on silicon," *Appl. Phys. Lett.*, vol. 104, no. 4, pp. 041104, Jan. 2014.

[16] S. Chen, M. Liao, M. Tang, J. Wu, M. Martin, T. Baron *et al.,* "Electrically pumped continuous-wave 1.3 µm InAs/GaAs quantum dot lasers monolithically grown on on-axis Si (001) substrates," *Opt. Express*, vol. 25, no. 5, pp. 4632–4639, Mar. 2017.

[17] D. Jung, J. Norman, M. J. Kennedy, C. Shang, B. Shin, Y. Wan *et al.*, "High efficiency low threshold current 1.3 µm InAs quantum dot lasers on on-axis (001) GaP/Si," *Appl. Phys. Lett.*, vol. 111, no. 12, pp. 122107, Sep. 2017.

[18] A. Y. Liu, J. Peters, X. Huang, D. Jung, J. Norman, M. L. Lee *et al.,* "Electrically pumped continuous-wave 1.3 µm quantum-dot lasers epitaxially grown on on-axis (001) GaP/Si," *Opt. Lett.*, vol. 42, no. 2, pp. 338–341, Feb. 2017.

[19] J. Norman, M. J. Kennedy, J. Selvidge, Q. Li, Y. Wan, A. Y. Liu *et al.,* "Electrically pumped continuous wave quantum dot lasers epitaxially grown on patterned, on-axis (001) Si," *Opt. Express*, vol. 25, no. 4, pp. 3927–3934, Feb. 2017.

[20] D. Jung, Z. Zhang, J. Norman, R. Herrick, M. J. Kennedy, P. Patel *et al.*, "Highly reliable low-threshold InAs quantum dot lasers on on-axis (001) Si with 87 % injection efficiency," ACS Photon., vol. 5, no. 3, pp 1094–1100, Mar. 2018.

[21] D. Inoue, D. Jung, J. Norman, Y. Wan, N. Nishiyama, S. Arai *et al.*, "Directly modulated 1.3 µm quantum dot lasers epitaxially grown on silicon," *Opt. Express*, vol. 26, no. 6, pp. 7022–7033, Mar. 2018.

[22] S. Liu, D. Jung, J. C. Norman, M. J. Kennedy, A. C. Gossard, J. E. Bowers, "490 fs pulse generation from passively mode-locked single section quantum dot laser directly grown on on-axis GaP/Si," *Electron. Lett.*, vol. 54, no. 7, pp. 432–433, Apr. 2018.

[23] M. Tang, S. Chen, J. Wu, Q. Jiang, V. G. Dorogan, M. Benamara *et al.,* "1.3-µm InAs/GaAs quantum-dot lasers monolithically grown on Si substrates using InAlAs/GaAs dislocation filter layers," *Opt. Express*, vol. 22, no. 10, pp. 11528–11535, May 2014.

[24] Z. Mi, J. Yang, P. Bhattacharya, G. Qin, and Z. Ma, "High-performance quantum dot lasers and integrated optoelectronics on Si," in *Proc. of the IEEE,* vol. 97, no 7, pp. 1239–1249, July 2009.

[25] J. Yoon, S. M Lee, D. Kang, M. A. Meitl, C. A. Bower, and J. Rogers, "Heterogeneously integrated optoelectronic devices enabled by micro-transfer printing," *Adv. Opt. Materials*, vol. 3, no. 10, pp. 1313–1335, Sep. 2015.

[26] A. Miller, D. T. Reid, and D. M. Finlayson, "Short pulse generation using semiconductor lasers," in *Ultrafast Photonics,* UK: CRC Press, 2004, pp. 43–58.

[27] J. C. Norman, D. Jung, Y. Wan, and J. E. Bowers, "Perspective: The future of quantum dot photonic integrated circuits," *APL Photon.*, vol. 3, no. 3, pp. 030901-01–030901-20, Mar. 2018.

[28] P. P. Vasil'ev, I. H. White, and J. Gowar, "Fast phenomena in semiconductor lasers," *Rep. Prog. Phys.*, vol. 63, no. 12, pp. 1997–2042, Oct. 2000.

[29] I. H. White, D. F. G. Gallagher, M. Osiński, and D. Bowley, "Direct streak-camera observation of picosecond gain-switched optical pulses from a 1.5 µm semiconductor laser," *Electron. Lett.*, vol. 21, no. 5, pp. 197–199, Feb. 1985.

[30] P. Downey, J. Bowers, R. Tucker, and E. Agyekum, "Picosecond dynamics of a gain-switched InGaAsP laser," *IEEE J. Quantum Electron.*, vol. 23, no. 6, pp. 1039–1047, Jun. 1987.

[31] D. Bimberg, K. Ketterer, E. H. Böttcher, and E. Schöll, "Gain modulation of unbiased semiconductor lasers: ultrashort light-pulse generation in the 0.8 µm-1.3 µm wavelength range," *Int. J. Electronics*, vol. 60, no. 1, pp. 23–45, Jun. 1986.

[32] R. A. Elliott, H. DeXiu, R. K. DeFreez, J. M. Hungt, and P. G. Rickman, "Picosecond optical pulse generation by impulse train current modulation of a semiconductor laser," *Appl. Phys. Lett.*, vol. 42, no. 12, pp. 1012–1014, June 1983.

[33] H. F. Liu, M. Fukazawa, Y. Kawai, and T. Kamiya, "Gain-switched picosecond pulse (< 10 ps) generation from 1.3 mu m InGaAsP laser diodes," *IEEE J. Quantum Electron.*, vol. 25, no. 6, pp. 1417–1425, June 1989.

[34] S. Schuster and H. Haug, "Analysis of emission and gain saturation in gain-switched semiconductor lasers," *JOSA B*, vol. 13, no. 7, pp. 1605–1613, July 1996.

[35] T.-P. Lee and R. H. Roldan, "Repetitively Q-switched light pulses from GaAs injection lasers with tandem double-section stripe geometry," *IEEE J. Quantum Electron.*, vol. 6, no. 6, pp. 339–352, June 1970.

[36] K. A. Williams, M. G. Thompson, and I. H. White, "Long-wavelength monolithic mode-locked diode lasers," *New. J. Phys.*, vol. 6, no. 1, pp. 179, Nov. 2004.

[37] A. R. Rae, M. G. Thompson, R. V. Penty, and I. H. White, "Dynamic simulation of mode-locked quantum-dot lasers," at *CLEO*, San Jose, CA, USA, 2008, p. CThF1.

[38] T. W. Berg, J. Mørk, and J. M. Hvam, "Gain dynamics and saturation in semiconductor quantum dot amplifiers," *New. J. Phys.*, vol. 6, no. 1, pp. 178, Nov. 2004.

[39] M. Gioannini and M. Rossetti, "Time-domain traveling wave model of quantum dot DFB lasers," *IEEE J. Sel. Top. Quantum Electron.,* vol. 17, no. 5, pp. 1318–1326, Sept-Oct. 2011.

[40] T. W. Berg and J. Mørk, "Saturation and noise properties of quantum-dot optical amplifiers," *IEEE J. Sel. Top. Quantum Electron.,* vol. 40, no. 11, pp. 1527–1539, Nov. 2004.

[41] A. Fiore and A. Markus, "Differential gain and gain compression in quantum-dot lasers," *IEEE J. Quantum Electron.*, vol. 67, no. 20, pp. 287–294, April 2007.

[42] J. Carroll, J. Whiteaway, and D. Plumb, "Numerical modelling for DFB lasers," in *Distributed Feedback Lasers,* London, UK: IET, 1998, pp. 209–251.

[43] R. Nagarajan, T. Fukushima, M. Ishikawa, J. E. Bowers, R. S. Geels, and L. A. Coldren, "Transport limits in high-speed quantum-well lasers: experiment and theory," *IEEE Photon. Technol. Lett.*, vol. 4, no. 2, pp. 121–123, Feb. 1992.

[44] J. Huang, and L. W. Casperson, "Gain and saturation in semiconductor lasers," *Opt. Quant. Electron.*, vol. 25, no. 6, pp. 369–390, Jan. 1993.

[45] M. Yamada and Y. Suematsu, "Analysis of gain suppression in undoped injection lasers," *J. Appl. Phys.*, vol. 52, no. 4, pp. 2653–2664, Aug. 1980.

[46] S. Mukai and H. Yajima, "Analysis of mode behavior in a waveguide with graded index and gain," *IEEE J. Quantum Electron.*, vol. 20, no. 7, pp. 728–733, July 1984.

[47] N. Hatori, M. Sugawara, K. Mukai, Y. Nakata, and H. Ishikawa, "Room-temperature gain and differential gain characteristics of self-assembled InGaAs/GaAs quantum dots for 1.1–1.3 µm semiconductor lasers," *Appl. Phys. Lett.*, vol. 77, no. 6, pp. 773–775, Aug. 2000.

[48] D. Arsenijević and D. Bimberg, "Quantum-dot lasers for 35 Gbit/s pulse-amplitude modulation and 160 Gbit/s differential quadrature phase-shift keying," in *Proc. SPIE Vol. 9892*, Brussels, Belgium, 2016, pp. 98920S.

[49] L. A. Coldren, S. W. Corzine, and M. L. Mashanovitch, "A phenomenological approach to diode lasers," in *Diode Lasers and Photonic Integrated Circuits,* New York, NY, USA: John Wiley & Sons, 2012, pp. 28–64.

[50] D. G. Deppe, H. Huang, and O. B. Shchekin, "Modulation characteristics of quantum-dot lasers: The influence of p-type doping and the electronic density of states on obtaining high speed," *IEEE J. Quantum Electron.*, vol. 39, no. 21, pp. 1587–1593, Dec. 2002.

0733-8724 (c) 2018 IEEE. Personal use is permitted, but republication/redistribution requires IEEE permission. See http://www.ieee.org/publications_standards/publications/rights/index.html for more information.